Biomicrofluidics

AIP Publishing

RESEARCH ARTICLE | NOVEMBER 16 2023

# Gas transport mechanisms through gas-permeable membranes in microfluidics: A perspective

Sangjin Seo ; Taesung Kim

*Biomicrofluidics* 17, 061301 (2023)
https://doi.org/10.1063/5.0169555

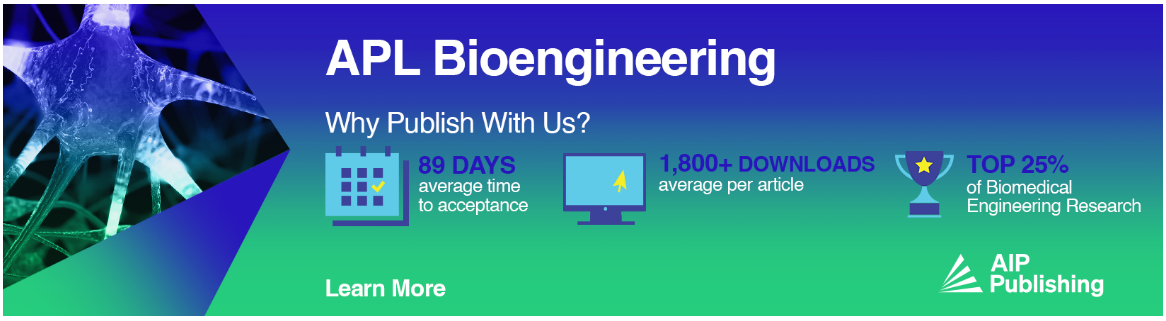

Biomicrofluidics PERSPECTIVE pubs.aip.org/aip/bmf

# Gas transport mechanisms through gas-permeable membranes in microfluidics: A perspective

Cite as: Biomicrofluidics **17**, 061301 (2023); doi: 10.1063/5.0169555
Submitted: 26 July 2023 · Accepted: 30 October 2023 ·
Published Online: 16 November 2023

Sangjin Seo[1] and Taesung Kim[1,2,a)]

## AFFILIATIONS

[1] Department of Mechanical Engineering, Ulsan National Institute of Science and Technology (UNIST), 50 UNIST-gil, Ulsan 44919, Republic of Korea
[2] Department of Biomedical Engineering, Ulsan National Institute of Science and Technology (UNIST), 50 UNIST-gil, Ulsan 44919, Republic of Korea

[a)] **Author to whom correspondence should be addressed:** tskim@unist.ac.kr. **Tel.:** +82-52-217-2313. **Fax:** +82-52-217-2409

## ABSTRACT

Gas-permeable membranes (GPMs) and membrane-like micro-/nanostructures offer precise control over the transport of liquids, gases, and small molecules on microchips, which has led to the possibility of diverse applications, such as gas sensors, solution concentrators, and mixture separators. With the escalating demand for GPMs in microfluidics, this Perspective article aims to comprehensively categorize the transport mechanisms of gases through GPMs based on the penetrant type and the transport direction. We also provide a comprehensive review of recent advancements in GPM-integrated microfluidic devices, provide an overview of the fundamental mechanisms underlying gas transport through GPMs, and present future perspectives on the integration of GPMs in microfluidics. Furthermore, we address the current challenges associated with GPMs and GPM-integrated microfluidic devices, taking into consideration the intrinsic material properties and capabilities of GPMs. By tackling these challenges head-on, we believe that our perspectives can catalyze innovative advancements and help meet the evolving demands of microfluidic applications.

## I. INTRODUCTION

Microfluidics has traditionally favored liquid-based devices, primarily due to the significant advantages offered by viscosity-dominant physics. The introduction of gases has often been avoided owing to the complexities arising from gas compression and inertia. Additionally, gas diffusion through channel walls presents unexpected challenges because of gas permeation. In contrast, the use of thin, gas-permeable membranes (GPMs) enables the controlled permeation of gases, facilitating rapid changes in the physiochemical conditions of microfluidic systems and guiding mass transport between gases and liquids. By incorporating gases, microfluidics moves beyond a mere liquid-based system and encompasses the complete essence of "fluid." This Perspective outlines the diverse range of applications and advantages associated with the utilization of gases in microfluidics.

The integration of gases in microfluidics serves various purposes across different fields of study. In the realm of biology, for instance, the presence of oxygen is crucial in terms of nutrient supply for the culture of cells, tissues, and organs.[1,2] Consequently, on-chip methods for manipulating oxygen delivery and creating oxygen concentration gradients have been developed.[3–5] Another critical demand is the monitoring of oxygen concentration.[5,6] In the field of chemistry, gas–liquid reactions enable precise control over gas–liquid volumes, gas–liquid interface areas, flow rates, and bubble sizes.[7,8] Physics and engineering have harnessed the unique characteristics of bubbles, which exhibit robust responses to diverse stimuli.[9] Furthermore, the study of two-phase flows yielded insights into the complexities of interfaces[10] and nonlinear behavior.[11] Additionally, the innovative concept of "aerofluidics" emerged, enabling the underwater manipulation of gases.[12] Evaporation and condensation processes also garnered significant attention in the fields of nanofluidics,[13] botany,[14] and energy.[15] Whether employed for fundamental research or practical applications, the key values of controllability and rapid response are inherent to microfluidics.

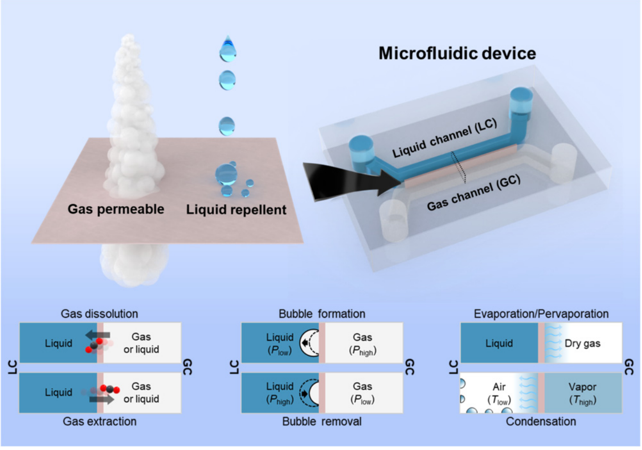

**FIG. 1.** Integration of GPMs into microfluidic devices for controlled gas transport (top). Transport mechanisms through GPMS are categorized into three representative groups: gas dissolution/extraction, bubble formation/removal, and evaporation/pervaporation/condensation (bottom).

GPMs effectively partition interfaces, enabling diffusion-based transport. Moreover, the emergence of GPMs with high transport rates and selective permeability offers ample opportunities for expanding the boundaries of microfluidic applications.

Gas transport mechanisms through GPMs can be categorized based on the direction and nature of the transported molecules, as illustrated in Fig. 1. A typical microfluidic device comprises a liquid channel, a gas channel, and a GPM that acts as a separator. In some cases, an environmental system can replace the gas channel, and a device wall made of gas-permeable material can be used in lieu of the GPM. In such setups, gas molecules either "dissolve" into the liquid channel or are "extracted" in the reverse direction, while those that dissolve slowly or do not dissolve lead to the formation and removal of "foam" bubbles at the liquid–GPM interface. Vapor molecules of the liquid exhibit behavior similar to that of gas molecules; they can evaporate or pervaporate through the GPM facilitating diffusive transport of vapor molecules. The introduction of vapor into the gas channel allows for "condensation" in a dry liquid channel by promoting the diffusion of vapor molecules. The specific types of transport are determined by various factors, including pressure differences, gas solubility, gas–GPM interactions, membrane roughness, humidity, and temperature. In this Perspective, we focus on the efficient utilization of gases in microfluidics, with a primary emphasis on microfluidic devices integrated with GPMs. After outlining various transport categories and their representative applications, we delve into the fundamental theories that explain these transport phenomena. We also conduct comparative analysis of GPMs based on their inherent properties and intended applications, highlighting the importance of emerging gas-selective GPM technologies in advancing microfluidics.

## II. MICROFLUIDIC APPLICATIONS OF GPMs

We classified the transport mechanisms into three distinct groups, taking into consideration the types of penetrant, namely, dissolving gases, bubbles, and vapors. Furthermore, each of these categories was further subdivided into two subcategories depending on the directionality between the liquid channel and the gas channel. In this section, we provided a concise overview of the associated phenomena, discussed methods for enhancing transport within microfluidic devices, and highlighted pertinent applications. Additionally, we included a summary of relevant publications since 2013 in Table I. Our classification is as follows:

### A. Dissolution and extraction of gases

When gas molecules diffuse from the gas channel, they can be absorbed by liquids and incorporated into the solution. The absorbed gases may either remain stable by retaining their molecular structure or dissociate into smaller parts. Unreactive gases, such as nitrogen ($N_2$), oxygen ($O_2$) in water, and noble gases, tend to remain stable once dissolved. However, when reactive gases, such as carbon dioxide ($CO_2$) or ammonia ($NH_3$), dissolve in water, they react with water molecules to produce ions. Generally, gases that dissociate have a greater capacity to dissolve compared to unreactive gases.[48] The diffusion rate and direction between the gas channel and the liquid channel can be modulated by controlling the concentration gradient along GPMs. Once gases are dissolved, they are contained in the liquid and carried by flow. Therefore, liquids can act as carriers, containers, and reactors for gas molecules. For example, blood oxygenators were developed by increasing the surface area for gas exchange with the aim of eventually meeting certain clinical criteria [Fig. 2(a)].[20] For practical utilization, it is necessary to simultaneously facilitate the dissolution of $O_2$ and the extraction of $CO_2$, surpassing respiratory consumption and production rates of these gases. Recently, an 8-layer oxygenator demonstrated *in vivo* animal testing for 24 h, maintaining a high oxygen transfer rate (27 ml of $O_2$/min) while meeting clinical criteria for pressure drops.[53] For a chemical reaction, tube-in-tube reactors represent a stepwise gas–liquid reaction in a microfluidic system [Fig. 2(b)].[7,49,54] A tube made of a gas-permeable polymer was inserted into another tube to enable controlled chemical reactions via effectively induced dissolution of gas. Additionally, gas mixtures were separated on a microfluidic device by utilizing GPMs with different gas permeabilities.[18] Gas dissolution is frequently used to maintain and modulate chemical conditions in liquids. For example, the levels of $O_2$ and $CO_2$ were maintained in microfluidic devices during cell, tissue, and organ culture.[5,55] Furthermore, $CO_2$ and $NH_3$ gas channels were designed to modulate the pH of the liquid channel [Fig. 2(c)].[50] These multilayer microfluidic channels enabled on-site sourcing of molecules while still confining the liquid within viscous-dominant microchannels. Concentration gradients of gases are more useful than constant concentration conditions to investigate the diverse responses at different conditions on a single device.[56]

Conversely, dissolved gases sometimes need to be extracted from the liquid. This requires an opposite concentration gradient. Flushing gases can be delivered into the gas channel to achieve this; however, maintaining a steep concentration gradient can be challenging as gas extraction increases the concentration of the gas channel. Therefore, gas-absorbing materials can be utilized to achieve a high extraction rate. For instance, $O_2$ gas was absorbed by

**TABLE I.** Summary of transport mechanisms and GPMs used in microfluidics.

| Classification | Material | Target gas | Application demonstrated | Integration | Support | Reference |
|---|---|---|---|---|---|---|
| Gas dissolution | 2.0-$\mu$m porous polycarbonate (PC) | Gaseous odorants | Gas sensing | … | PDMS | 16 |
| | Hydrogel | $O_2$ | Cell culture | Gelation | Glass | 17 |
| | PDMS | $CO_2$ | Gas removal | Plasma bonding | PDMS | 8 |
| | PDMS | $CO_2$ | Solution analysis | Thermocompression | PMMA | 19 |
| | PDMS | $O_2$ | Oxygenation | Plasma bonding | Self-standing | 20 |
| | Photocurable PDMS resin | $O_2$ | … | Stereolithography | Self-standing | 21 |
| | Porous PDMS | $CO_2$ | Glucose synthesis | PDMS gluing | PDMS | 22 |
| | Porous PTFE membrane | Formaldehyde | Gas sensing | Adhesive | PDMS | 23 |
| Gas dissolution/extraction | 38-nm porous anodized aluminum oxide (AAO) | Air | Cell culture | Micromachining | Silicon | 24 |
| | 0.1-$\mu$m, 0.05-$\mu$m porous PC, porous PDMS, PDMS | $O_2$, $CO_2$ | Oxygenation | PDMS gluing | PDMS | 25 |
| | 0.22-$\mu$m porous polyvinylidene fluoride (PVDF) | $SO_2$, $HNO_2$, $CO_2$ | Gas sensing | Lamination | Cyclic olefin copolymer (COC) | 26 |
| | PDMS | $CO_2$ | … | Chemical bonding | PMMA | 27 |
| | PDMS | $O_2$ | Gas sensing | Clamping | PDMS/low temperature co-fired ceramic (LTCC) | 28 |
| | PDMS in a PTFE scaffold | $O_2$, $CO_2$ | Oxygenation | PDMS gluing | PDMS | 29 |
| | Porous PTFE membrane | $NH_3$ | Gas sensing | Lamination | Paper | 30 |
| | Teflon AF2400 | Various gases | Tube-in-tube reactor | Tubing | PTFE tubing | 7 |
| Extraction | 0.45-$\mu$m porous PTFE membrane | $SO_2$ | Gas sensing | Adhesive/lamination | Paper | 31 |
| | Porous PTFE membrane | $SO_2$ | Gas sensing | Adhesive | Stacked tape | 32 |
| Bubble removal | 0.2-$\mu$m porous PTFE membrane | Air | Bubble removal | Adhesive | Polypropylene film | 33 |
| | 0.45-$\mu$m, 1.0-$\mu$m, 1.0-$\mu$m, 3.0-$\mu$m porous PTFE membrane | Air | Bubble removal | Adhesive | Polyimide film | 34 |
| | 10-$\mu$m porous PTFE membrane | Air | Bubble removal | Adhesive lamination | PMMA, polyester film | 35 |
| | Liquid-infused porous membrane | Air | Bubble removal | Clamping | PMMA | 36 |
| | PDMS | Air | Filling dead-end volume | Casting | PE | 37 |
| | PDMS | Air | Membrane formation | Plasma bonding | PDMS | 38 |
| | PDMS | Air | Bubble removal | Plasma bonding | PET | 39 |
| Pervaporation | x-PDMS | Water | Particle assembly | Plasma bonding/chemical bonding | PDMS/Ostemer 324 Flex | 40 |
| | PDMS | Ethanol | Ethanol removal | Plasma bonding | PDMS | 41 |
| | PDMS | Acetone | Acetone removal | Plasma bonding | Glass | 42 |
| Evaporation | 0.2–0.5-$\mu$m porous expanded PTFE (ePTFE) membrane | Water | Heat sink | Adhesive | Porous copper | 43 |
| | 2.4-$\mu$m porous silicon-rich silicon nitride (SiRN) | Water | Sample concentration | Micromachining | Silicon | 44 |
| | 5–30-$\mu$m porous PTFE membrane | Water | Sample crystallization | PDMS gluing | PDMS | 45 |
| Pervaporation/condensation | x-PDMS/PDMS | Water | Molecular transport control | Polymerization/plasma bonding | PDMS/glass | 46 |
| Evaporation/condensation | 1-$\mu$m PTFE powder | Water | Refilling of liquid marbles | … | Powder layer | 47 |

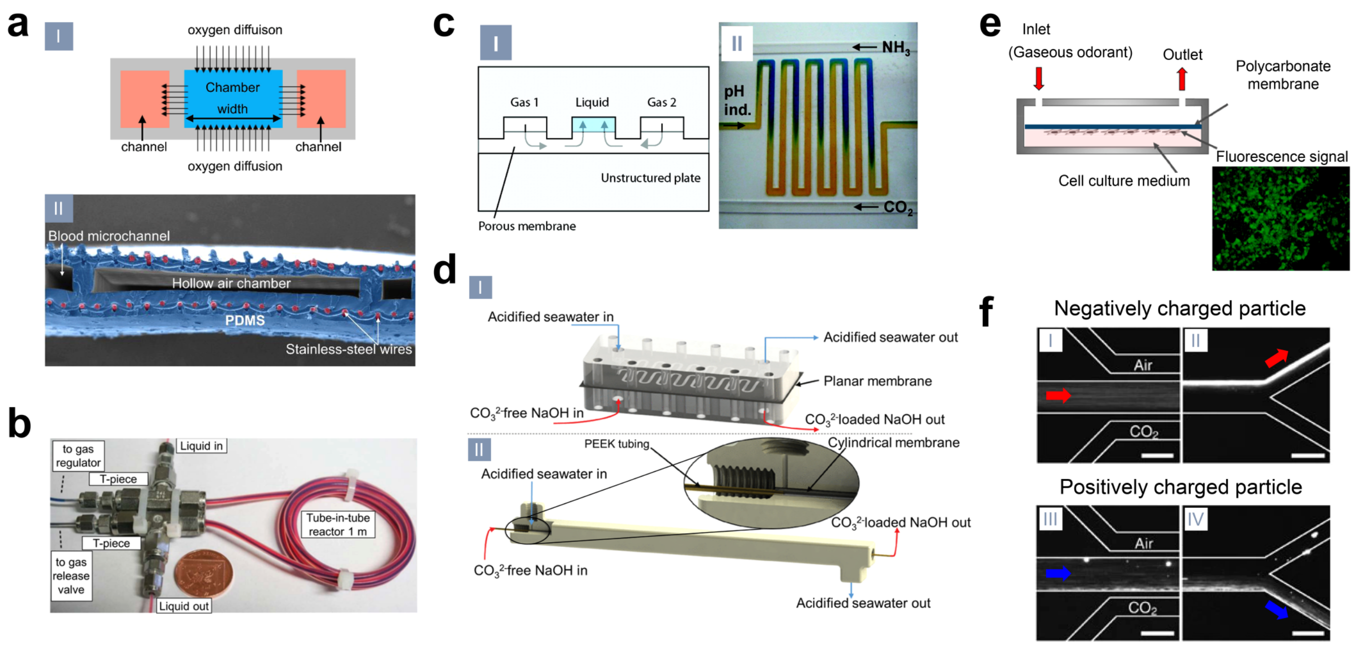

FIG. 2. Diffusive gas transport via GPM for various microfluidic applications. (a) Mimicking $O_2$ dissolution into a blood vessel using a microfluidic channel network with an optimized surface-volume ratio.[20] Reproduced with permission from Dabaghi *et al.*, J. Membr. Sci. **596**, 117741 (2020). Copyright 2020 Elsevier. (b) A tube-in-tube reactor consisting of a liquid-flow tube inside a gas-flow tube.[49] The inner tube allows gas permeability for gas transport between the liquid and gas flows. Reproduced with permission from Browne *et al.*, Synlett **23**(09), 1402–1406 (2012). Copyright 2012 Thieme. (c). Manipulation of the pH of the liquid flow in a microchannel by dissolving acidic $CO_2$ and basic $NH_3$ gases.[50] Reproduced with permission from de Jong *et al.*, Anal. Chem. **80**(9), 3190–3197 (2008). Copyright 2008 American Chemical Society. (d) $CO_2$ concentration measurement from sea water by extracting $CO_2$ gas from the top sample channel to the bottom collecting channel.[51] Reproduced with permission from P. J. Bresnahan and T. R. Martz, IEEE Sens. J. **18**(6), 2211–2217 (2018). Copyright 2018 IEEE. (e). Cell-based fluorescent probe for detection of gaseous odorant on a chip.[16] Reproduced with permission from Lee *et al.*, Biosens. Bioelectron. **74**, 554–561 (2015). Copyright 2015 Elsevier. (f) Generation of a concentration gradient of $CO_2$ across a microchannel for diffusiophoretic particle separation.[52] The migration direction across the microchannel depends on the surface charge of particles. Reproduced with permission from Shin *et al.*, Nat. Commun. **8**, 15181 (2017). Copyright 2017 Author(s), licensed under a Creative Commons Attribution (CC BY) license.

$O_2$ scavenger solution—pyrogallol/sodium hydroxide (NaOH) solution—via a polydimethylsiloxane (PDMS) wall and continuously consumed by a reaction to maintain a steep concentration gradient.[57] Similarly, toxic gases produced in a reaction can be simultaneously extracted and dissolved into a parallel channel filled with a reactant.[58] This simultaneous process prevents the leakage of toxic gases via distillation. Furthermore, sequential chemical reactions can be designed on a centrifugal microfluidic platform by incorporating gas diffusion into the process.[26] Gas extraction is also used to analyze gaseous components in liquids. As shown in Fig. 2(d), gases can be extracted before being delivered to a sensing unit, such as in the cases of sensing $CO_2$ in seawater,[19,51] sulfur dioxide ($SO_2$) gas in wine,[31,59] or $O_2$ and $NH_3$ in samples.[28,30] Each unit incorporated electrical or optical sensing mechanisms to facilitate on-chip determination, thereby reducing time and labor costs. In certain instances, gas-reactive biological cells can serve as biosensors that exhibit fluorescence signals on the dissolution of target odorant molecules [Fig. 2(e)].[16] Unlike other sensors, cell-based biosensors can switch their target gas molecules using different types of cells while retaining sensing selectivity. They require only simple calibration to establish the relationship between gas concentration and signal intensity.

A concentration gradient of gas molecules can be generated within a liquid-flowing channel, with the dissolution channel acting as the source and the extraction channel functioning as the destination. For instance, a pair of a source and a sink can be used to generate a $CO_2$ gradient in the flow of cell culture media.[60] Additionally, a $CO_2$ concentration gradient can be harnessed for the removal of particles in a low-energy water filtration process [Fig. 2(f)].[52] The dissolved $CO_2$ molecules dispersed along the liquid stream create a pronounced ion concentration gradient across the channel, thereby prompting the diffusiophoretic migration of particles based on their surface charges and sizes. Furthermore, the distinct diffusiophoretic velocities of these particles facilitate their separation, which is contingent upon surface properties.[61]

### B. Formation and removal of bubbles

The presence of bubbles in a liquid has a significant impact on the entire fluid network, giving rise to bubble logic[62] and fluidic actuators.[63] Additionally, bubbles can serve as carriers of encapsulated gases and shell materials, thereby facilitating their applications across various fields.[9,64,65] Within a microfluidic system, bubbles can be generated through several mechanisms, including multiphase

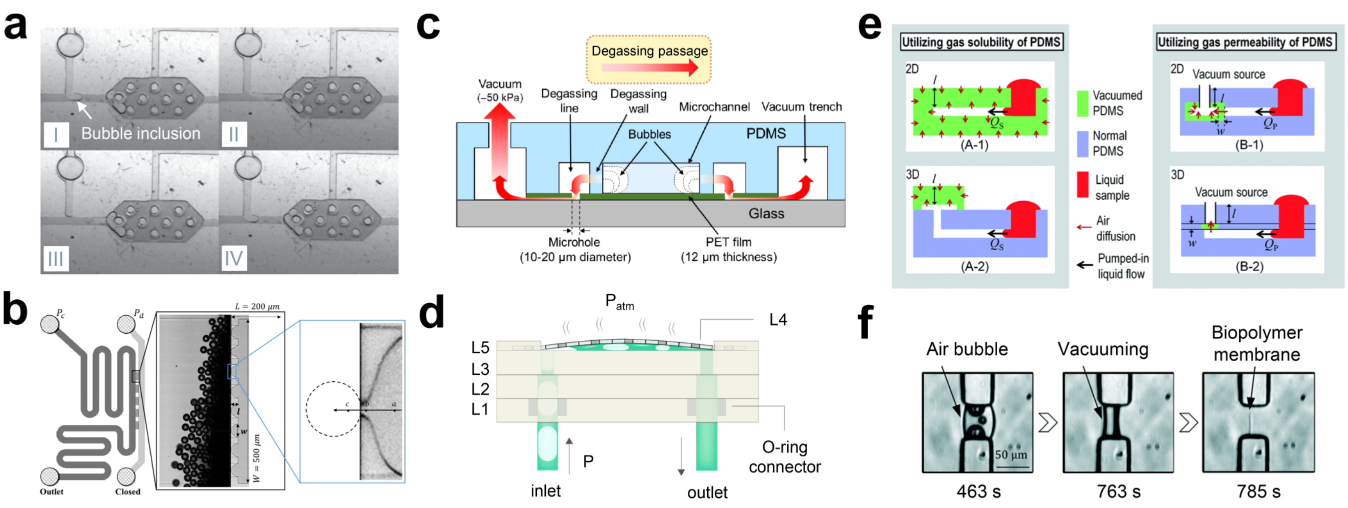

**FIG. 3.** Gas transport in the form of bubbles and its microfluidic applications. (a) Bubble formation under higher gas pressure across a PDMS membrane.[72] Reproduced with permission from Johnson *et al.*, J. Micromech. Microeng. **19**(9), 095011 (2009). Copyright 2009 IOP Publishing. (b) Bubble formation via a hydrophilic porous structure, generating monodisperse bubbles.[73] Reproduced with permission from Deng *et al.*, J. Colloid Interface Sci. **622**, 218–227 (2022). Copyright 2022 Elsevier. (c) Bubble removal in the liquid by applying a vacuum on the opposite sidewalls of the central liquid channel made of PDMS.[39] Reproduced with permission from Park *et al.*, Membranes **11**(5), 316 (2021). Copyright 2021 Author(s), licensed under a Creative Commons Attribution (CC BY) license. (d) Inlet pressure drives flow and evacuates bubbles through the membrane when a bubble–liquid mixture passes through the gap channel between the deflected porous membrane and the rigid wall.[35] Reproduced with permission from Williams *et al.*, Micromachines **10**(6), 360 (2019). Copyright 2019 Author(s), licensed under a Creative Commons Attribution (CC BY) license. (e) Filling dead-end structures using various vacuum sources, resulting in air removal. Pre-vacuumed PDMS absorbs air inside the dead-end structures or vacuum sources are applied to the opposite side of a thin PDMS membrane.[74] Reproduced with permission from Xu *et al.*, Lab Chip **15**(20), 3962–3979 (2015). Copyright 2015 Royal Society of Chemistry. (f) Guided formation of a biopolymer membrane by removing trapped bubbles for *in situ* membrane fabrication.[38] When two solutions are positioned on opposite sides of a bubble and deliberately brought into contact, a controlled polymerization process takes place. Reproduced with permission from Pham *et al.*, Lab Chip **17**(2), 248–255 (2017). Copyright 2017 Royal Society of Chemistry.

flow,[66] electrolysis,[67] chemical reactions,[68] cavitation-induced nucleation,[69] and physical stimuli using acoustic, optical, or thermal energy.[69] An alternative approach involves applying high gas pressure across GPMs to induce bubble formation within the liquid. These bubbles can maintain their size if the bubble is stabilized by a shell made of surfactants, lipids, or hydrophobic materials.[70,71] Positive or negative pressure can be applied to a PDMS membrane to produce or remove bubbles, respectively [Fig. 3(a)].[72] Bubble inclusions could be applied for a bubble-based gating mechanism. However, the utilization of a nonporous membrane is restricted to basic operations due to challenges in controlling bubble size. Instead, by employing a microchannel membrane (i.e., porous membrane), high-speed imaging for the growth of uniformly sized bubbles can be achieved. This enables analytic studies in well-confined geometries [Fig. 3(b)].[73] The dynamic interfacial behavior was investigated to determine the effect of protein adsorption during bubble formation. Furthermore, efforts are being made to realize high-throughput monodisperse bubble formation using microchannel membranes.[75] Furthermore, membrane-based bubble formation might be highly valuable in situations requiring on-the-spot bubble formation. For instance, bubble-based perfusion in culture chambers[76] would be controlled in a localized and individual manner using membrane-based bubble formation.

Generally, GPMs are more commonly used for bubble removal rather than bubble formation. Both unintentionally and intentionally formed bubbles need to be eliminated once they have fulfilled their purpose.[69,77,78] Failure to remove these bubbles can result in their adhesion to walls, leading to increased hydrodynamic resistance and nonlinearity in the fluidic system.[11] Bubble removal devices have been comprehensively reviewed in recent papers.[69,77–79] Therefore, we specifically focus on membrane-based bubble removal in this Perspective article. Bubble removal in continuous flow has been developed for use as a pre- or post-treatment component. Bubbles can be evacuated through dense membranes or hydrophobic porous membranes by creating a pressure difference across the membranes. Dense PDMS membranes are employed when a vacuum can be applied to the device [Fig. 3(c)].[39] The PDMS-based bubble removal channel can be integrated as either a pre- or post-component in a multi-step microfluidic device. Furthermore, the feasibility of using a vacuum eliminates the necessity for applying high pressure to the liquid. Structural optimization, such as incorporating a bubble trap,[72] a sloped structure,[80] or a longer channel,[39] can enhance bubble removal via dense membranes. In contrast, when aiming for higher removal rates, hydrophobic porous membranes are integrated into microfluidic devices. Hydrophobic porous membranes can successfully remove bubbles without requiring a vacuum.[33,34] As demonstrated in Fig. 3(d), a device solely dedicated to bubble removal achieved a high removal rate (1.5 ml/min) while maintaining a compact size ($10 \times 18.5 \times 6\ \text{mm}^3$ for width × length × height).[35] Although the flow rate becomes complex upon connection with another microfluidic device, the independently operating module is convenient and cost-effective. An exceptional example involves the use of liquid-infused membranes, which facilitate anti-fouling bubble removal.[36] Furthermore, the combination of membranes with different bubble wettability has demonstrated the proof of concept for microfluidic bubble removal.[81] Bubble removal also aided in filling dead-end pores [Fig. 3(e)].[74] The presence of air in these dead-end pores was reduced by bubble removal, allowing liquids to occupy the volume quickly. Additionally, pre-vacuumed polymers can absorb air without the need for vacuum application after liquid loading, thereby eliminating the need for additional gas channels. Guided bubble removal can be leveraged to fabricate controlled interfaces of biopolymer membranes [Fig. 3(f)].[38] Applying a vacuum to stably trapped bubbles in the absence of liquid flow eliminated the need for intricate pressure balancing to prevent pressure fluctuations during membrane growth. Notably, gas diode membranes exhibited directionality in bubble transport, which can be employed in microfluidic devices for stepwise chemical reactions.[68]

### C. Evaporation, pervaporation, and condensation of solutions

A porous membrane enables continuous evaporation while maintaining the gas–liquid interface within its pores. Various methods can be employed to enhance the rate of evaporation. Typically, a refreshing gas flow was used to maintain a steep vapor concentration gradient.[44] Thermal energy can also be utilized to facilitate evaporation [Fig. 4(a)].[45] The porous membrane served as a pathway for vapor and offered a stable gas–liquid interface for crystal growth. Similarly, an effective evaporation technique concentrated the solution, leading to a rapid concentration of samples containing short-lived radiolabeled tracers.[83] Another option for an evaporative membrane entails the adoption of a dense material, such as PDMS. Microfluidic devices composed of dense material have gas-permeable walls, which permit evaporation through them (i.e., pervaporation). However, the millimeter-scale thickness of the channel wall lowers the concentration gradient and restricts severe pervaporation. Over prolonged periods, such as during cell incubation, pervaporation can significantly increase osmolarity.[84] To address water loss, common solutions include humidifying the entire incubation system or placing an "iso-osmotic bath."[85] In contrast, when there is a high surface-to-volume ratio and a thin dense membrane, pervaporation becomes effective enough to be a dominant phenomenon. Solvent mixture separation via pervaporation is achieved in channels that are hundreds of millimeters in length [Fig. 4(b)].[42] The removal efficiency was studied using 2D numerical simulation, taking into account the advection in the nominal direction due to permeation flux, thereby elucidating the

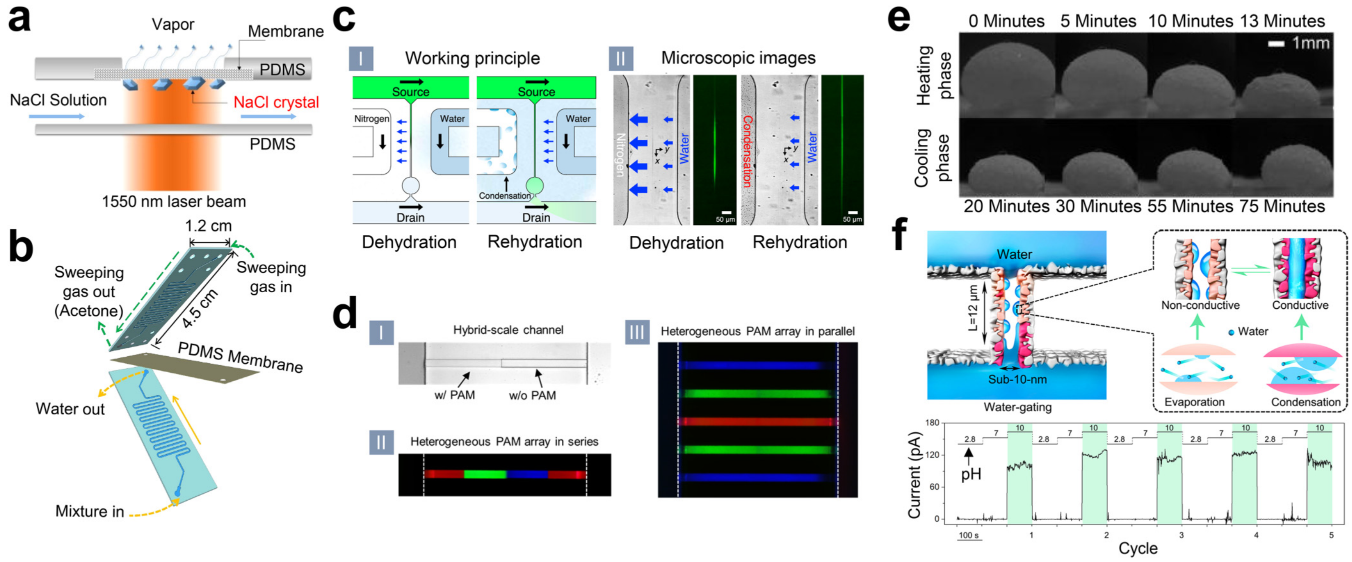

**FIG. 4.** Solvent transport with a phase change for various microfluidic applications. (a) Microfluidic local evaporator for crystallization of NaCl. Robust evaporation facilitated by laser-induced thermal energy and a porous membrane enabling crystallization of highly diffusive salt.[45] Reproduced with permission from He *et al.*, Sep. Purif. Technol. **242**, 116817 (2020). Copyright 2020 Elsevier. (b) Separation of a water–acetone mixture using two parallel channels separated by a PDMS membrane.[42] Reproduced with permission from Zhang *et al.*, Chem. Eng. J. **284**, 1342–1347 (2016). Copyright 2016 Elsevier. (c) Locally controlled pervaporation near a nanoslit for molecular transport control.[46] Repeatable switching between dehydration and rehydration actuates liquid transport in a reversible manner. Reproduced with permission from Seo *et al.*, Nat. Commun. **12**, 1336 (2021). Copyright 2021 Author(s), licensed under a Creative Commons Attribution (CC BY) License. (d) Pervaporation-induced flow migrates particles along the channel and assembles them at the target location.[40] Stepwise migration and assembly of various particles enable the fabrication of heterogeneous particle structures in various forms. Reproduced with permission from Seo *et al.*, Lab Chip **22**(8), 1474–1485 (2022). Copyright 2022 Royal Society of Chemistry. (e) Evaporation and condensation of liquid marbles, where the resulting liquid volumes vary, depending on the temperature condition.[47] Reproduced with permission from Sreejith *et al.*, Appl. Phys. Lett. **120**(6), 064102 (2022). Copyright 2022 AIP Publishing LLC. (f) Liquid gating of a nanopore actuated by evaporation and condensation. The pH-mediated gating of the nanopore is demonstrated by current signals.[82] Reproduced with permission from Xiao *et al.*, ACS Nano **10**(10), 9703–9709 (2016). Copyright 2016 American Chemical Society.

reason for the limitation in removal efficiency. Pervaporation also enables solute concentration in confined structures, allowing for low concentrations to reach their saturation concentration.[86] A similar mechanism in a longitudinal microchannel provides a valuable tool for analyzing the mutual diffusion of binary solution.[87]

Furthermore, the continuity of liquid generates pervaporation-induced flow.[88] Leveraging this mechanism, a simple microfluidic pump was initially designed by mimicking leaves.[89] Subsequently, flow generation becomes locally and independently controllable by designing individual control channels for liquid channels, enabling various dynamic functions, such as molecular concentrators, pumps, and filters [Fig. 4(c)].[46] Numerical and experimental studies showed that the advection caused by the pervaporation-induced flow is sufficient to compare with diffusion of small molecules. Pervaporation-induced flow was also utilized to assemble particles [Fig. 4(d)].[40] The particle assemblies exhibit a porous structure that enables solvent penetration, thereby ensuring that the evaporation area remains constant. As a result, the assembly rate remains rapid even as the particle assembly grows and occupies a larger volume. Then, the particle assembly served as a homogeneous/heterogeneous nanoporous membrane whose pore properties are determined by the particle properties, including pore size, functional group, and wettability. This methodology of particle assembly has been employed for several applications, including transport control of small molecules,[40] solidification of colloidal dispersion,[90] and plasmonic supercrystals.[91]

In addition, condensation offers reverse working principles of pervaporation, and water supply through a GPM can be leveraged to collect water from the environment. Microfluidic channels can simplify the phenomena,[92] and GPMs can serve as both walls and an all-around vapor source for fluidic channels. However, controlling on-chip vapor condensation is often challenging owing to its unpredictable nature. Only in a few cases is the condensation considered for manipulating liquids in microfluidics. For example, liquid marbles covered with hydrophobic powder can be refilled through condensation via cooling [Fig. 4(e)].[47] Although the condensation process is much slower than the evaporation process, condensation-based refilling offers a potential method for noninvasive volume recovery of a liquid marble. Similarly, a humid environment facilitates the reconnection of disconnected channels filled with hydrophilic fluorescent molecules.[46] Furthermore, we believe that the controllability of liquid connection via evaporation and condensation holds potential for gating mechanisms.[82] Membrane-based condensation may enable humidity-based gating, in contrast to the pH control proposed in Fig. 4(f). For example, dissolutions of acidic/basic gases can provide similar pH control in nanopores, while humidification of the gases can accelerate capillary condensation. Moreover, water harvesting structures,[93] guided transportation,[94] and self-humidifying membranes[95] can be employed to collect water from the environment, increasing responsiveness to environmental conditions for humidity-dependent actuations.

## D. Summary

In summary, transport of gases through GPMs in microfluidic devices offers a range of possibilities depending on types of penetrants and the specific system designed to guide them. These transport phenomena have been utilized in numerous ways, serving as the foundation for sophisticated microfluidic applications. The use of gases enables dynamic changes within liquid systems, affecting driving forces, actuation, and chemical stimuli. This dynamism includes rapid condition changes, repeatability, and the reversibility of these changes. The integration of a membrane enhances the device's practicality, either with or without interfacial pores. Thin membranes are fabricated and integrated to induce a higher gradient of chemical potential across them, thereby increasing the transport rate. Additionally, the thin structure reduces the device's volume, enhancing its responsiveness to changing conditions, albeit sometimes requiring a minimum volume for adequate gas absorption. Furthermore, the gas selectivity of GPMs opens up possibilities for unique applications that go beyond the functions based solely on the nature of the penetrants. However, certain applications, such as bubble formation and condensation, have been explored only to the extent of demonstrating their feasibility. Even for other gas transport mechanisms, recent developments do not appear to significantly diversify away from the previous research achievements. To overcome this challenge, it is necessary to focus on the type of GPM employed. By carefully selecting GPMs, high permeability or selective gas transports can be achieved, which enables devices to possess greater robustness and reduced size while maintaining the same performance. In light of these considerations, we conducted a concise yet comprehensive investigation into GPMs, aiming to provide guidance for their utilization in the field of microfluidics.

## III. BASIC TRANSPORT MECHANISMS THROUGH GPMs

GPMs can be designed and fabricated in either dense or porous forms. In this section, we provided a summary of fundamental theories from a microfluidics-focused perspective, complemented by schematics presented in Fig. 5. It is worth noting that we do not discuss the integration of GPMs into microfluidic devices, which has already been extensively covered in the previous literature.[96–98]

## A. Dense membranes

Dense membranes are nonporous and devoid of interconnected pore networks, and gas molecules transport solely through diffusion, as illustrated in Fig. 5(a). Gas transport via dense membranes follows the solution–diffusion model.[99] Gas molecules are considered to jump from one free-volume to another.[100–102] The solution–diffusion transport of gas species through a dense membrane can be expressed as follows:[99]

$$N_g = \bar{P}_g \frac{\Delta p_g}{L},$$

$$\bar{P}_g = S_g \cdot D_g,$$

where $N_g$ is the permeation flux of a gas through a dense membrane, $\bar{P}_g$ [barrer, 1 barrer = $1 \times 10^{-10}$ cm$^3$ (STP) cm/(cm$^2$ s cmHg)] is the permeability coefficient of a gas through a dense membrane, $\Delta p_g$ is the partial pressure difference of a gas across the membrane, $L$ is the membrane thickness, $S_g$ [cm$^3$ (STP)/(cm$^3$ cmHg)] is the

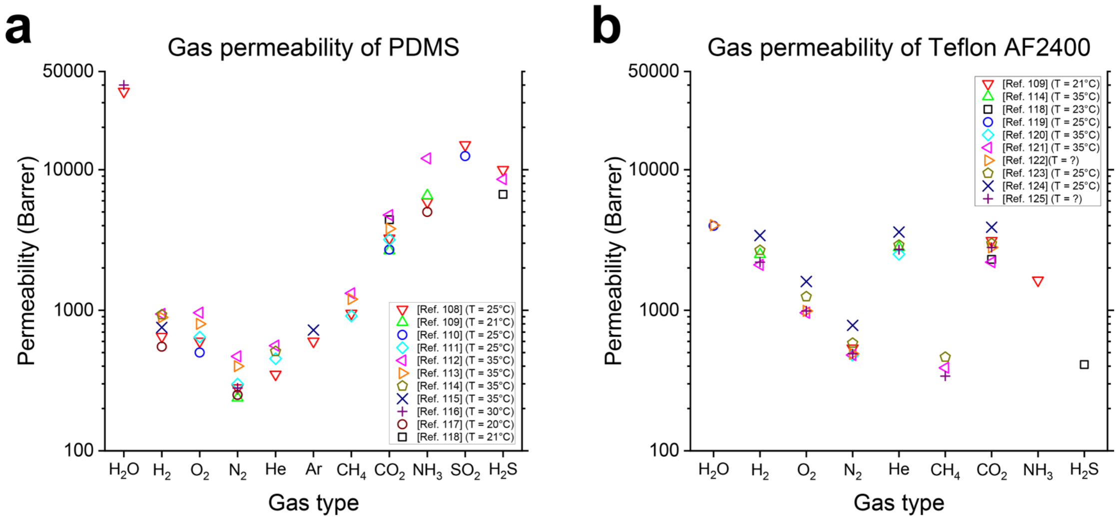

**FIG. 5.** Gas transport mechanisms facilitated by conventional GPMs, specifically highlighting the process of gas dissolution through the membranes. (a) The transportation of gaseous molecules involves sorption, diffusion, and desorption stages as they traverse the dense membrane. Gas permeability ($\bar{P}_g$) is determined by the multiplication of the solubility coefficient ($S_g$) and the diffusivity ($D_g$) of the gas. (b) A hydrophobic porous membrane (when $d > \lambda$) maintains a gas–liquid interface in the case of a higher liquid pressure, owing to the capillary entry pressure ($p_e$). Therefore, the intermembrane transport of gas molecules predominantly relies on gas diffusion. (c) A hydrophilic porous membrane (when $d > \lambda$) holds potential for GPMs when appropriate precautions are taken into consideration prior to use. Gas molecules undergo dissolution into the liquid phase prior to traversing the membrane pore, leading to retarded intermembrane transport. A porous membrane stably maintains the gas–liquid interface when the pressure difference ($\Delta p = p_{nwp} - p_{wp}$) is smaller than the capillary entry pressure ($p_e$).

solubility coefficient of a gas into a dense membrane, and $D_g$ is the diffusivity of a gas through a dense membrane.

There exists a reciprocal correlation between the permeation and selectivity. Therefore, the trade-offs between the permeability and selectivity of gases in homogeneous polymer membranes have been extensively studied.[103,104] Although originally formulated for homogeneous polymer membranes, the trade-off relation offers insight for evaluating various types of GPMs, including porous membranes, and serves as an initial guideline for selecting a suitable GPM for specific microfluidic applications. However, as indicated in Table I, the range of available GPMs for microfluidic devices is indeed limited. For dense membranes, PDMS is commonly employed because of its excellent performance in gas separation and high permeability for specific gases, particularly water. Nonetheless, this limits the application to the inherent selectivity of the PDMS membrane itself. Hence, there are new functionalities to be unlocked by incorporating the gas selectivity of other membranes, which can enhance microfluidic systems. For instance, improved gas selectivity and permeability can enhance the performance of sensing devices in terms of selectivity and robustness. Furthermore, selective collection of reactants in chemical and biological processes becomes feasible, enabling stepwise and segregated processes.

Notably, when dealing with mixed-gas environments, relying solely on permeability data from individual gases may not always yield accurate results. Gas selectivity in a mixture can differ from the ideal gas selectivity calculated based on individual gas permeabilities.[105] Like temperature, humidity plays a significant role in the permeability of gases, including vapor itself.[106,107] While the pressure effect on permeability is generally negligible in the typical pressure range in microfluidics. In Fig. 6, the gas permeabilities of PDMS[108–118] and Teflon AF2400[109,114,118–125] were investigated from literature studies. Both materials are commercially available and well known for their high gas permeability.[114,126] The high permeability is a prerequisite in microfluidic applications because moderate working pressures are acceptable; otherwise, the microfluidic device undergoes deformation or rupture at high pressure. PDMS is a silicon-based rubbery polymer and is one of the most frequently used GPMs in microfluidics due to its mechanical properties, biocompatibility for microfluidics, and accumulated knowledge in fabrication and modifications.[127] As shown in Fig. 6(a), PDMS has high gas permeabilities and even higher water permeability.[114,126] Furthermore, PDMS has a hydrophobic nature with extremely low water solubility. However, PDMS exhibits anomalously high permeability, while Bian *et al.* recently suggested an explanation by hydrogen-bonded chains of nanoscopically confined water.[126]

Teflon AF2400 is a fluorocarbon-based glassy polymer. As a fluorocarbon-based polymer, Teflon AF2400 also demonstrates high permeability, as shown in Fig. 6(b). The $O_2$ and $CO_2$ gas permeabilities of Teflon AF2400 are comparable to those of PDMS, implying that Teflon AF2400 membranes have the potential for use in cell culture systems.[128] Therefore, Teflon AF2400 can be a PDMS alternative when similar $O_2$ and $CO_2$ gas permeability is required, but water permeation is prohibited. Furthermore, the chemical and mechanical durability of Teflon AF2400 enables the use of organic solvents without significant swelling and permeation.[123,129] Teflon AF2400 is commercially available in a variety of

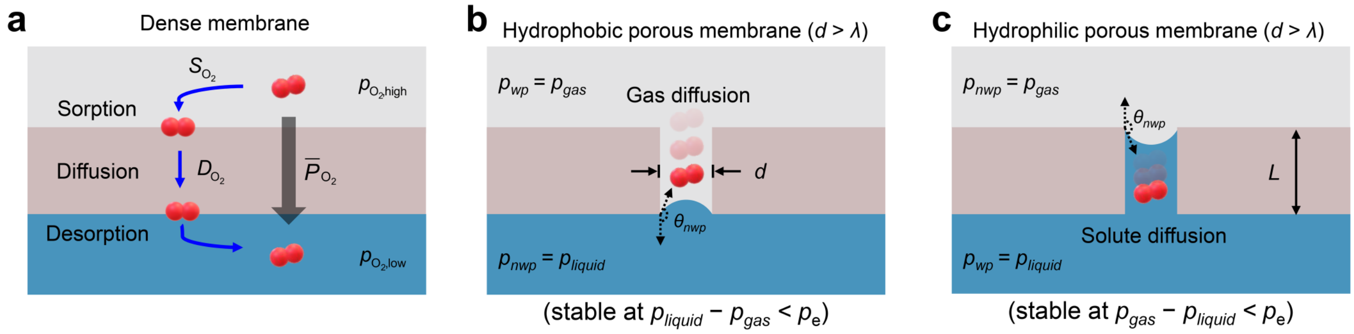

**FIG. 6.** Permeabilities of various gases used in microfluidic devices from several literature works. (a) PDMS. (b) Teflon AF2400.

forms. In particular, tubular Teflon AF2400 membranes have inspired a new concept of fluidic platform, i.e., the aforementioned "tube-in-tube reactor."[7,54] In addition to the above two materials, there are several popular alternatives for dense membranes. For example, poly[1-trimethylsilyl-1-propyne] (PTMSP) is popular for its ultrahigh permeability,[130] and polyimide is likewise popular for its excellent gas selectivity.[104]

## B. Porous membranes

Essentially, no gas selectivity is realized by the porous membrane when its pore size ($d$) surpasses the mean free path of penetrants ($\lambda$); for air, $\lambda = 64$–$68$ nm at room temperature and atmospheric pressure.[131] This implies that, if $d > \lambda$, sophisticated gas–membrane interactions in the ambient condition can be neglected.

Assisted by hydrophobicity, porous membranes do not allow for the pressure-driven permeation of liquid into the gaseous pores of the membrane up to a certain critical pressure [Fig. 5(b)]. In other words, the gas–liquid interface in the membrane pores can be stably maintained when the pressure difference between two phases ($\Delta p = p_{nwp} - p_{wp}$, where $p_{nwp}$ is the pressure of a non-wetting phase and $p_{wp}$ is that of a wetting phase) is lower than the capillary entry pressure ($p_e$) in the membrane pores,[132]

$$p_e = \frac{4\gamma \cos(\pi - \theta_{nwp})}{d},$$

where $\gamma$ is the gas–liquid surface tension and $\theta_{nwp}$ is the contact angle between a non-wetting phase and a solid. The maximum pore size ($d_m$) can be calculated using the interfacial properties of the liquid, gas, and membrane. For example, for a polytetrafluoroethylene (PTFE) membrane, the $d_m = \frac{123\ (\text{kPa}\cdot\mu\text{m})}{p}$ is derived from the literature data ($\gamma = 72.75 \times 10^{-3}$ N/m and $\theta = 115°$).[133] Therefore, for hydrophobic porous membranes, pore sizes are acceptable even up to tens of micrometers under appropriate liquid pressures. Notably, the capillary entry pressure is influenced by several geometrical factors, such as membrane thickness, surface roughness, and pore shape.[132,134,135] Surfactants, which are widely used in microfluidics, induce the wetting of the pores and consequently reduce the capillary entry pressure, emphasizing the need for superhydrophobic/omniphobic membranes.[136] The intramembrane transport of gases is governed by Fick's law. The transport along membrane pores is not exactly governed by the same mechanism as the gas diffusion occurring at ambient gas–liquid interfaces because of the membrane porosity ($\varepsilon$) and tortuosity ($\tau$) determining the effective diffusion coefficient ($\overline{D} = \varepsilon D/\tau$), where $D$ is the diffusion coefficient. Furthermore, it is worth noting that effective diffusion flux varies upon the diffusive direction because of the anisotropic tortuosity of membrane pores.[137]

On the other hand, hydrophilic membranes should be utilized to prevent the absorbance of hydrophobic molecules[138] or adopt surface modification for biocompatibility.[139] In the case of a hydrophilic membrane, an additional strategy is required to prevent pressure-driven permeation [Fig. 5(c)]. The gas pressure should be higher than the liquid pressure to maintain the gas–liquid interface, facilitating bubble generation.[73] Smaller pores within a hydrophilic membrane can stabilize the gas–liquid interface in both directions of a pressure gradient.[24] However, there are several critical issues that require careful consideration. The lack of a thin structure poses challenges for the membrane to effectively mitigate transport of gases, resulting in a significant reduction in transport rates. As illustrated in Fig. 5(c), this reduction is primarily attributed to the additional diffusion resistance presented by the liquid barrier within the hydrophilic membrane.[140] Moreover, hydrophilic membrane pores are susceptible to small fluctuations of surroundings or condensation, thereby causing complete wetting of the pores and subsequent pressure-driven permeation. Therefore, the utilization of hydrophilic membranes for GPMs is only valid when a stable gas–liquid interface is guaranteed during the operation of a microfluidic device.

The intermediate transport behavior of dense and porous membranes can be achieved by reducing the pore size of the porous membrane. When the pore size becomes smaller than the mean free path (i.e., $d < \lambda$), it results in selective gas transport, driven by several phenomena, namely, *Knudsen diffusion*, *surface diffusion*, *capillary condensation*, and *molecular sieving*. These transport processes occurring at the pore level are inherently mixed, even within a single pore, and this situation varies simultaneously from pore to pore.[141] Detailed mechanisms of transport and the origin of selectivity are extensively covered in the existing literature.[142–144] Building upon the intermediate performance achieved by balancing gas selectivity and permeability through these phenomena, numerous GPMs have emerged and continue to be developed. Section IV delves into these GPMs and explores their potential for utilization in microfluidics.

## IV. GAS-SELECTIVE GPMs FOR MICROFLUIDICS

We offer an overview of newly emerging gas-selective GPMs, with a specific focus on membrane technology and microfluidic applications of gas separation. This on-chip gas separation is poised to make a significant impact in the field of microfluidics, promising precise and efficient processing of gas and liquid within microfluidic platforms.

Recent advancements in membrane technology aim to address the perennial challenge of striking the right balance between permeability and selectivity. In response to this challenge, novel membrane materials, such as polymers of intrinsic microporosity (PIMs) and thermally rearranged (TR) polymers, have been developed. These super-glassy polymers exhibited exceptional performance, albeit with certain durability limitations. Researchers are actively exploring innovative strategies to overcome these obstacles.[145,146] Notably, the ionization of polymers has been employed to further enhance membrane properties.[147] Additionally, heterogeneous membranes have been introduced, including thin-film composite (TFC) membranes[148] and mixed-matrix membranes (MMMs).[149] TFC membranes involve the formation or deposition of an ultrathin dense polymer layer onto a rigid membrane support, enabling the simultaneous integration of the selectivity of dense membranes and the mechanical strength of the support layer. MMMs, on the other hand, consist of organic polymers blended with inorganic additives to overcome the limitation of each. Generally, inorganic material improves gas selectivity, while polymers provide mechanical stability without losing the membrane role. The inorganic additives include zeolites, metal-organic frameworks (MOFs), nanocarbons, and other nanoparticles. Furthermore, the heterogeneous membranes utilize the other emerging polymers, such as PIMs and TRs.[145,150,151]

To date, various types of membranes have been developed for diverse gas separation applications, including gas–gas separation, dehumidification, and pervaporation separation.[145–152] However, their suitability for microfluidics may be limited. This is mainly due to challenges in achieving improved permeability of gases with highly selective membranes, which are crucial for miniaturization and robust processing, the core aims of microfluidics. Emerging gas-selective membranes offer the potential to specifically enhance precision and efficiency in microfluidic applications. Furthermore, there are still several advantages in microfluidics when utilized for gas separation. Serial placement of GPMs in a microfluidic device realized miniaturized serial gas processing flow.[54] A high surface-to-volume ratio reduces the amount of samples required and allows for supporting liquid solutions, such as enzyme, to work effectively.[18] The application of selective membranes allows for the pre-separation of sample gases, effectively eliminating interfering gases that may produce similar signals to the target gas or disrupt the sensing mechanism.[153] Additionally, these membranes enable the retention or removal of gaseous cellular by-products, such as nitric oxide (NO) and methane ($CH_4$), while facilitating the transport of $O_2$ and $CO_2$. Such selective control of gaseous components within a liquid environment can be beneficial for studying the impact of by-products on cell culturing within a gas-controlled microfluidic device. This approach enables a shift in focus from idealized scenarios where only single gases are considered, to more realistic situations involving mixtures of multiple gases. By incorporating emerging gas-selective membranes into microfluidic platforms, researchers gain the capability to explore and manipulate complex gas mixtures, thereby advancing the understanding and application of gas-related processes in diverse fields.

Last, it is important to acknowledge that the integration of emerging gas-selective membranes into microfluidics is not without challenges. The development of easy and cost-effective fabrication methods for on-chip integration is a crucial aspect that needs to be addressed. Furthermore, investigations on the compatibility of these membranes with the physiochemical environment of microfluidics and their interaction with biomolecules are essential.[154] Also, the requirement for transparency in observations imposes limitations on the selection of membranes. Additionally, inherent issues associated with certain membranes, such as aging and plasticization, must be addressed as important considerations. Despite the barriers that need to be overcome, it is evident that the infinite combination of gases and liquids undoubtedly enriches the field of microfluidics. Continued research and development in this area holds tremendous potential for further advancements and innovations in gas-related processes within the microfluidic domain.

## V. CONCLUSIONS AND OUTLOOK

We categorized gas transport mechanisms in microfluidics into three distinct groups: the dissolution and extraction of gases, the formation and removal of gas bubbles, and the evaporation and condensation of solutions. Our exploration delved into the fundamental mechanisms of GPMs and provided a comprehensive review of their recent applications, drawing upon a wealth of literature from the realm of microfluidics. In particular, GPM-based gas transport offers numerous advantages, especially in scenarios where rapid switching of physiochemical conditions and on-site molecule transport into or from liquids within devices is desired. While the literature discussed here predominantly emphasizes the transport itself and the ensuing physiochemical phenomena, there exists a profound connection to potential biological applications. Beyond merely regulating $O_2/CO_2$ levels for cell culture, GPMs open the door to precise molecule delivery within a fluidic network—a capability of paramount importance. Gating mechanisms, such as bubble inclusion and capillary evaporation, can be harnessed for the targeted delivery of drugs, signaling molecules, and nanoparticles. Particle migration methods, such as diffusiophoresis and pervaporation-induced flow, can similarly be applied to cells, facilitating the transport of vital biological materials, such as nucleic acids, proteins, and liposomes. These dynamic mechanisms provide researchers with powerful tools for conducting intricate biological experiments within microchannels, similar to those traditionally conducted in cell culture plates. Furthermore, another promising application lies in the assembly of antibody-tagged particles for simultaneous detection. Moreover, emulating the fluidic system in plants not only enables the replication of their microfluidic capabilities, but also allows for a comprehensive understanding through the utilization of devices that offer advantages in manipulating parameters, such as geometry, contact angle, and environmental conditions.[155,156] However, despite these compelling advantages and promising applications, we have observed stagnation in the development and innovation of GPM-based microfluidic applications. Our analysis has indicated that a dearth of diversity in available membranes, specifically scarcity of polymer choices, severely restricts the range of gases and liquids that can be selectively transported. To overcome this limitation, it is imperative that we foster a deeper understanding of both conventional and emerging membrane technologies. By increasing the diversity of GPMs, we can significantly broaden the scope of microfluidic applications and fully unlock the potential of liquid and gas manipulation within microfluidic systems. We believe that by expanding our knowledge in this area, we can usher in a new era of innovation and transformative applications in microfluidics.

## ACKNOWLEDGMENTS

This work was supported by the National Research Foundation of Korea (NRF) grant funded by the Korean government (MSIT) (NRF-2020R1A2C3003344). This work was also supported by the Technology Innovation Program (Development of Underwater Breathing Device Technology without An Oxygen Tank, 20026073) funded by the Ministry of Trade, Industry & Energy (MOTIE) of Korea.

## AUTHOR DECLARATIONS

### Conflict of Interest

The authors have no conflicts to disclose.

### Author Contributions

**Sangjin Seo:** Conceptualization (lead); Writing – original draft (lead); Writing – review & editing (equal). **Taesung Kim:** Conceptualization (equal); Funding acquisition (lead); Supervision (lead); Writing – review & editing (equal).

## DATA AVAILABILITY

Data sharing is not applicable to this article as no new data were created or analyzed in this study.

## REFERENCES

[1] C. M. Leung, P. de Haan, K. Ronaldson-Bouchard, G.-A. Kim, J. Ko, H. S. Rho, Z. Chen, P. Habibovic, N. L. Jeon, S. Takayama, M. L. Shuler, G. Vunjak-Novakovic, O. Frey, E. Verpoorte, and Y.-C. Toh, "A guide to the organ-on-a-chip," Nat. Rev. Methods Primers **2**, 33 (2022).

[2] J. M. Ayuso, M. Virumbrales-Munoz, J. M. Lang, and D. J. Beebe, "A role for microfluidic systems in precision medicine," Nat. Commun. **13**, 3086 (2022).

[3] V. Palacio-Castaneda, N. Velthuijs, S. Le Gac, and W. P. R. Verdurmen, "Oxygen control: The often overlooked but essential piece to create better *in vitro* systems," Lab Chip **22**(6), 1068–1092 (2022).

[4] M. D. Brennan, M. L. Rexius-Hall, L. J. Elgass, and D. T. Eddington, "Oxygen control with microfluidics," Lab Chip **14**(22), 4305–4318 (2014).

[5] K. R. Rivera, M. A. Yokus, P. D. Erb, V. A. Pozdin, and M. Daniele, "Measuring and regulating oxygen levels in microphysiological systems: Design, material, and sensor considerations," Analyst **144**(10), 3190–3215 (2019).

[6] M. Azimzadeh, P. Khashayar, M. Amereh, N. Tasnim, M. Hoorfar, and M. Akbari, "Microfluidic-based oxygen [O(2)] sensors for on-chip monitoring of cell, tissue and organ metabolism," Biosensors **12**(1), 6 (2022).

[7] M. Brzozowski, M. O'Brien, S. V. Ley, and A. Polyzos, "Flow chemistry: Intelligent processing of gas-liquid transformations using a tube-in-tube reactor," Acc. Chem. Res. **48**(2), 349–362 (2015).

[8] M. Abolhasani, A. Gunther, and E. Kumacheva, "Microfluidic studies of carbon dioxide," Angew. Chem., Int. Ed. **53**(31), 7992–8002 (2014).

[9] Y. Li, X. Liu, Q. Huang, A. T. Ohta, and T. Arai, "Bubbles in microfluidics: An all-purpose tool for micromanipulation," Lab Chip **21**(6), 1016–1035 (2021).

[10] C.-X. Zhao and A. P. J. Middelberg, "Two-phase microfluidic flows," Chem. Eng. Sci. **66**(7), 1394–1411 (2011).

[11] S. Battat, D. A. Weitz, and G. M. Whitesides, "Nonlinear phenomena in microfluidics," Chem. Rev. **122**(7), 6921–6937 (2022).

[12] J. Yong, Y. Peng, X. Wang, J. Li, Y. Hu, J. Chu, and D. Wu, "Self-driving underwater 'aerofluidics,'" Adv. Sci. **10**, 2301175 (2023).

[13] J. Zhong, M. A. Alibakhshi, Q. Xie, J. Riordon, Y. Xu, C. Duan, and D. Sinton, "Exploring anomalous fluid behavior at the nanoscale: Direct visualization and quantification via nanofluidic devices," Acc. Chem. Res. **53**(2), 347–357 (2020).

[14] K. H. Jensen, K. Berg-Sørensen, H. Bruus, N. M. Holbrook, J. Liesche, A. Schulz, M. A. Zwieniecki, and T. Bohr, "Sap flow and sugar transport in plants," Rev. Mod. Phys. **88**(3), 035007 (2016).

[15] C. Chen, Y. Kuang, and L. Hu, "Challenges and opportunities for solar evaporation," Joule **3**(3), 683–718 (2019).

[16] S. H. Lee, E. H. Oh, and T. H. Park, "Cell-based microfluidic platform for mimicking human olfactory system," Biosens. Bioelectron. **74**, 554–561 (2015).

[17] F. Bunge, S. Driesche, and M. Vellekoop, "Microfluidic platform for the long-term on-chip cultivation of mammalian cells for lab-on-a-chip applications," Sensors **17**(7), 1603 (2017).

[18] M. Malankowska, C. F. Martins, H. S. Rho, L. A. Neves, R. M. Tiggelaar, J. G. Crespo, M. P. Pina, R. Mallada, H. Gardeniers, and I. M. Coelhoso, "Microfluidic devices as gas–ionic liquid membrane contactors for $CO_2$ removal from anaesthesia gases," J. Membr. Sci. **545**, 107–115 (2018).

[19] M. Tweedie, D. Sun, D. R. Gajula, B. Ward, and P. D. Maguire, "The analysis of dissolved inorganic carbon in liquid using a microfluidic conductivity sensor with membrane separation of CO(2)," Microfluid. Nanofluid. **24**(5), 37 (2020).

[20] M. Dabaghi, N. Saraei, G. Fusch, N. Rochow, J. L. Brash, C. Fusch, and P. R. Selvaganapathy, "Microfluidic blood oxygenators with integrated hollow chambers for enhanced air exchange from all four sides," J. Membr. Sci. **596**, 117741 (2020).

[21] E. Fleck, A. Sunshine, E. DeNatale, C. Keck, A. McCann, and J. Potkay, "Advancing 3D-printed microfluidics: Characterization of a gas-permeable, high-resolution PDMS resin for stereolithography," Micromachines **12**(10), 1266 (2021).

[22] X. Ren, H. Lu, J. G. Zhou, P. L.-G. Chong, W. Yuan, and M. Noh, "Porous polydimethylsiloxane as a gas–liquid interface for microfluidic applications," J. Microelectromech. Syst. **26**(1), 120–126 (2017).

[23] X. L. Guo, Y. Chen, H. L. Jiang, X. B. Qiu, and D. L. Yu, "Smartphone-based microfluidic colorimetric sensor for gaseous formaldehyde determination with high sensitivity and selectivity," Sensors **18**(9), 3141 (2018).

[24] F. Bunge, S. van den Driesche, and M. J. Vellekoop, "PDMS-free microfluidic cell culture with integrated gas supply through a porous membrane of anodized aluminum oxide," Biomed. Microdevices **20**(4), 98 (2018).

[25] W. I. Wu, N. Rochow, E. Chan, G. Fusch, A. Manan, D. Nagpal, P. R. Selvaganapathy, and C. Fusch, "Lung assist device: Development of microfluidic oxygenators for preterm infants with respiratory failure," Lab Chip **13**(13), 2641–2650 (2013).

[26] O. Ymbern, N. Sandez, A. Calvo-Lopez, M. Puyol, and J. Alonso-Chamarro, "Gas diffusion as a new fluidic unit operation for centrifugal microfluidic platforms," Lab Chip **14**(5), 1014–1022 (2014).

[27] M. Tweedie, D. Sun, B. Ward, and P. D. Maguire, "Long-term hydrolytically stable bond formation for future membrane-based deep ocean microfluidic chemical sensors," Lab Chip **19**(7), 1287–1295 (2019).

[28] J. Luo, T. Dziubla, and R. Eitel, "A low temperature co-fired ceramic based microfluidic Clark-type oxygen sensor for real-time oxygen sensing," Sens. Actuators B **240**, 392–397 (2017).

[29] M. Dabaghi, N. Saraei, G. Fusch, N. Rochow, J. L. Brash, C. Fusch, and P. R. Selvaganapathy, "An ultra-thin highly flexible microfluidic device for blood oxygenation," Lab Chip **18**(24), 3780–3789 (2018).

[30] B. M. Jayawardane, I. D. McKelvie, and S. D. Kolev, "Development of a gas-diffusion microfluidic paper-based analytical device (muPAD) for the determination of ammonia in wastewater samples," Anal. Chem. **87**(9), 4621–4626 (2015).

[31] M. Chen, H. Yang, L. Rong, and X. Chen, "A gas-diffusion microfluidic paper-based analytical device (muPAD) coupled with portable surface-enhanced Raman scattering (SERS): Facile determination of sulphite in wines," Analyst **141**(19), 5511–5519 (2016).

[32] P. Prasertying, T. Ninlapath, N. Jantawong, T. Wongpakdee, T. Sonsa-Ard, K. Uraisin, P. Saetear, P. Wilairat, and D. Nacapricha, "Disposable microchamber with a microfluidic paper-based lid for generation and membrane separation of SO(2) gas employing an *In situ* electrochemical Gas sensor for quantifying sulfite in wine," Anal. Chem. **94**(22), 7892–7900 (2022).

[33] Y. Cheng, Y. Wang, Z. Ma, W. Wang, and X. Ye, "A bubble- and clogging-free microfluidic particle separation platform with multi-filtration," Lab Chip **16**(23), 4517–4526 (2016).

[34] H. G. Derami, R. Vundavilli, and J. Darabi, "Experimental and computational study of gas bubble removal in a microfluidic system using nanofibrous membranes," Microsyst. Technol. **23**(7), 2685–2698 (2017).

[35] M. J. Williams, N. K. Lee, J. A. Mylott, N. Mazzola, A. Ahmed, and V. V. Abhyankar, "A low-cost, rapidly integrated debubbler (RID) module for microfluidic cell culture applications," Micromachines **10**(6), 360 (2019).

[36] X. Hou, Y. Hu, A. Grinthal, M. Khan, and J. Aizenberg, "Liquid-based gating mechanism with tunable multiphase selectivity and antifouling behaviour," Nature **519**(7541), 70–73 (2015).

[37] S. H. Lee, J. Song, B. Cho, S. G. Hong, O. Hoxha, T. Kang, D. Kim, and L. P. Lee, "Bubble-free rapid microfluidic PCR," Biosens. Bioelectron. **126**, 725–733 (2019).

[38] P. Pham, T. Vo, and X. Luo, "Steering air bubbles with an add-on vacuum layer for biopolymer membrane biofabrication in PDMS microfluidics," Lab Chip **17**(2), 248–255 (2017).

[39] S. Park, H. Cho, J. Kim, and K. H. Han, "Lateral degassing method for disposable film-chip microfluidic devices," Membranes **11**(5), 316 (2021).

[40] S. Seo, J. Bae, H. Jeon, S. Lee, and T. Kim, "Pervaporation-assisted *in situ* formation of nanoporous microchannels with various material and structural properties," Lab Chip **22**(8), 1474–1485 (2022).

[41] A. Zizzari, M. Bianco, E. Perrone, M. G. Manera, S. Cellamare, S. Ferorelli, R. Purgatorio, A. Scilimati, A. Tolomeo, V. Dimiccoli, R. Rella, and V. Arima, "Microfluidic pervaporation of ethanol from radiopharmaceutical formulations," Chem. Eng. Process.: Process Intensif. **141**, 107539 (2019).

[42] Y. Zhang, N. E. Benes, and R. G. H. Lammertink, "Performance study of pervaporation in a microfluidic system for the removal of acetone from water," Chem. Eng. J. **284**, 1342–1347 (2016).

[43] J. W. Palko, H. Lee, D. D. Agonafer, C. Zhang, K. W. Jung, J. Moss, J. D. Wilbur, T. J. Dusseault, M. T. Barako, F. Houshmand, G. G. Rong, T. Maitra, C. Gorle, Y. Won, D. Rockosi, I. Mykyta, D. Resler, D. Altman, M. Asheghi, J. G. Santiago, and K. E. Goodson, "High heat flux Two-phase cooling of electronics with integrated diamond/porous copper heat sinks and microfluidic coolant supply," in *2016 15th IEEE Intersociety Conference on Thermal and Thermomechanical Phenomena in Electronic Systems (ITherm)* (IEEE, 2016), pp. 1511–1517.

[44] H. Zhang, R. M. Tiggelaar, S. Schlautmann, J. Bart, and H. Gardeniers, "In-line sample concentration by evaporation through porous hollow fibers and micromachined membranes embedded in microfluidic devices," Electrophoresis **37**(3), 463–471 (2016).

[45] X. He, R. Chen, X. Zhu, Q. Liao, and S. Li, "Laser assisted microfluidic membrane evaporator for sample crystallization separation," Sep. Purif. Technol. **242**, 116817 (2020).

[46] S. Seo, D. Ha, and T. Kim, "Evaporation-driven transport-control of small molecules along nanoslits," Nat. Commun. **12**, 1336 (2021).

[47] K. R. Sreejith, P. Singha, N.-K. Nguyen, C. H. Ooi, D. V. Dao, and N.-T. Nguyen, "Noninvasive refilling of liquid marbles with water for microfluidic applications," Appl. Phys. Lett. **120**(6), 064102 (2022).

[48] E. Wilhelm, R. Battino, and R. J. Wilcock, "Low-pressure solubility of gases in liquid water," Chem. Rev. **77**(2), 219–262 (1977).

[49] D. Browne, M. O'Brien, P. Koos, P. Cranwell, A. Polyzos, and S. Ley, "Continuous-flow processing of gaseous ammonia using a Teflon AF-2400 tube-in-tube reactor: Synthesis of thioureas and in-line titrations," Synlett **23**(09), 1402–1406 (2012).

[50] J. de Jong, P. W. Verheijden, R. G. H. Lammertink, and M. Wessling, "Generation of local concentration gradients by gas-liquid contacting," Anal. Chem. **80**(9), 3190–3197 (2008).

[51] P. J. Bresnahan and T. R. Martz, "Gas diffusion cell geometry for a microfluidic dissolved inorganic carbon analyzer," IEEE Sens. J. **18**(6), 2211–2217 (2018).

[52] S. Shin, O. Shardt, P. B. Warren, and H. A. Stone, "Membraneless water filtration using $CO_2$," Nat. Commun. **8**, 15181 (2017).

[53] B. C. Isenberg, E. M. Vedula, J. Santos, D. J. Lewis, T. R. Roberts, G. Harea, D. Sutherland, B. Landis, S. Blumenstiel, J. Urban, D. Lang, B. Teece, W. Lai, R. Keating, D. Chiang, A. I. Batchinsky, and J. T. Borenstein, "A clinical-scale microfluidic respiratory assist device with 3D branching vascular networks," Adv. Sci. **10**(18), e2207455 (2023).

[54] R. Singh, H.-J. Lee, A. K. Singh, and D.-P. Kim, "Recent advances for serial processes of hazardous chemicals in fully integrated microfluidic systems," Korean J. Chem. Eng. **33**(8), 2253–2267 (2016).

[55] A. J. Mäki, M. Peltokangas, J. Kreutzer, S. Auvinen, and P. Kallio, "Modeling carbon dioxide transport in PDMS-based microfluidic cell culture devices," Chem. Eng. Sci. **137**, 515–524 (2015).

[56] J. F. Lo, E. Sinkala, and D. T. Eddington, "Oxygen gradients for open well cellular cultures via microfluidic substrates," Lab Chip **10**(18), 2394–2401 (2010).

[57] H. C. Shih, T. A. Lee, H. M. Wu, P. L. Ko, W. H. Liao, and Y. C. Tung, "Microfluidic collective cell migration assay for study of endothelial cell proliferation and migration under combinations of oxygen gradients, tensions, and drug treatments," Sci. Rep. **9**(1), 8234 (2019).

[58] R. A. Maurya, C. P. Park, J. H. Lee, and D. P. Kim, "Continuous *in situ* generation, separation, and reaction of diazomethane in a dual-channel microreactor," Angew. Chem., Int. Ed. **50**(26), 5952–5955 (2011).

[59] V. Kokoric, J. Theisen, A. Wilk, C. Penisson, G. Bernard, B. Mizaikoff, and J. P. Gabriel, "Determining the partial pressure of volatile components via substrate-integrated hollow waveguide infrared spectroscopy with integrated microfluidics," Anal. Chem. **90**(7), 4445–4451 (2018).

[60] S. P. Forry and L. E. Locascio, "On-chip $CO_2$ control for microfluidic cell culture," Lab Chip **11**(23), 4041–4046 (2011).

[61] T. J. Shimokusu, V. G. Maybruck, J. T. Ault, and S. Shin, "Colloid separation by $CO_2$-induced diffusiophoresis," Langmuir **36**(25), 7032–7038 (2020).

[62] M. Prakash and N. Gershenfeld, "Microfluidic bubble logic," Science **315**(5813), 832–835, (2007).

[63] Y. Gao, M. Wu, Y. Lin, and J. Xu, "Trapping and control of bubbles in various microfluidic applications," Lab Chip **20**(24), 4512–4527 (2020).

[64] A. Huerre, V. Miralles, and M. C. Jullien, "Bubbles and foams in microfluidics," Soft Matter **10**(36), 6888–6902 (2014).

[65] J. Mujtaba, J. Liu, K. K. Dey, T. Li, R. Chakraborty, K. Xu, D. Makarov, R. A. Barmin, D. A. Gorin, V. P. Tolstoy, G. Huang, A. A. Solovev, and Y. Mei, "Micro-bio-chemo-mechanical-systems: Micromotors, microfluidics, and nanozymes for biomedical applications," Adv. Mater. **33**(22), 2007465 (2021).

[66] A. Sattari, P. Hanafizadeh, and M. Hoorfar, "Multiphase flow in microfluidics: From droplets and bubbles to the encapsulated structures," Adv. Colloid Interface Sci. **282**, 102208 (2020).

[67] H. Kim, H. Hwang, S. Baek, and D. Kim, "Design, fabrication and performance evaluation of a printed-circuit-board microfluidic electrolytic pump for lab-on-a-chip devices," Sens. Actuators A **277**, 73–84 (2018).

[68] A. Gao, H. Fan, G. Zhang, S. Zhao, J. Cui, and Y. Yan, "Facile construction of gas diode membrane towards *in situ* gas consumption via coupling two chemical reactions," J. Colloid Interface Sci. **557**, 282–290 (2019).

[69] I. Pereiro, A. Fomitcheva Khartchenko, L. Petrini, and G. V. Kaigala, "Nip the bubble in the bud: A guide to avoid gas nucleation in microfluidics," Lab Chip **19**(14), 2296–2314 (2019).

[70] M. H. Lee, V. Prasad, and D. Lee, "Microfluidic fabrication of stable nanoparticle-shelled bubbles," Langmuir **26**(4), 2227–2230 (2010).

[71] E. Stride and M. Edirisinghe, "Novel microbubble preparation technologies," Soft Matter **4**(12), 2350 (2008).

[72] M. Johnson, G. Liddiard, M. Eddings, and B. Gale, "Bubble inclusion and removal using PDMS membrane-based gas permeation for applications in pumping, valving and mixing in microfluidic devices," J. Micromech. Microeng. **19**(9), 095011 (2009).

[73] B. Deng, K. Schroen, and J. de Ruiter, "Dynamics of bubble formation in spontaneous microfluidic devices: Controlling dynamic adsorption via liquid phase properties," J. Colloid Interface Sci. **622**, 218–227 (2022).

[74] L. Xu, H. Lee, D. Jetta, and K. W. Oh, "Vacuum-driven power-free microfluidics utilizing the gas solubility or permeability of polydimethylsiloxane (PDMS)," Lab Chip **15**(20), 3962–3979 (2015).

[75] Q. Shen, C. Zhang, M. F. Tahir, S. Jiang, C. Zhu, Y. Ma, and T. Fu, "Numbering-up strategies of micro-chemical process: Uniformity of distribution of multiphase flow in parallel microchannels," Chem. Eng. Process. Process Intensif. **132**, 148–159 (2018).

[76] A. Saleheen, D. Acharyya, R. A. Prosser, and C. A. Baker, "A microfluidic bubble perfusion device for brain slice culture," Anal. Methods **13**(11), 1364–1373 (2021).

[77] J. M. Karlsson, M. Gazin, S. Laakso, T. Haraldsson, S. Malhotra-Kumar, M. Maki, H. Goossens, and W. van der Wijngaart, "Active liquid degassing in microfluidic systems," Lab Chip **13**(22), 4366–4373 (2013).

[78] M. P. Yang, N. Sun, Y. Luo, X. C. Lai, P. R. Li, and Z. Y. Zhang, "Emergence of debubblers in microfluidics: A critical review," Biomicrofluidics **16**(3), 031503 (2022).

[79] C. Lochovsky, S. Yasotharan, and A. Gunther, "Bubbles no more: In-plane trapping and removal of bubbles in microfluidic devices," Lab Chip **12**(3), 595–601 (2012).

[80] C. Huang, J. A. Wippold, D. Stratis-Cullum, and A. Han, "Eliminating air bubble in microfluidic systems utilizing integrated in-line sloped microstructures," Biomed. Microdevices **22**(4), 76 (2020).

[81] J. Yong, J. Zhuang, X. Bai, J. Huo, Q. Yang, X. Hou, and F. Chen, "Water/gas separation based on the selective bubble-passage effect of underwater superaerophobic and superaerophilic meshes processed by a femtosecond laser," Nanoscale **13**(23), 10414–10424 (2021).

[82] K. Xiao, Y. Zhou, X. Y. Kong, G. Xie, P. Li, Z. Zhang, L. Wen, and L. Jiang, "Electrostatic-charge- and electric-field-induced smart gating for water transportation," ACS Nano **10**(10), 9703–9709 (2016).

[83] P. H. Chao, J. Collins, J. P. Argus, W. Y. Tseng, J. T. Lee, and R. Michael van Dam, "Automatic concentration and reformulation of PET tracers via microfluidic membrane distillation," Lab Chip **17**(10), 1802–1816 (2017).

[84] R. Mukhopadhyay, "When PDMS isn't the best: What are its weaknesses, and which other polymers can researchers add to their toolboxes?," Anal. Chem. **79**(9), 3248–3253 (2007).

[85] V. Lecault, M. Vaninsberghe, S. Sekulovic, D. J. H. F. Knapp, S. Wohrer, W. Bowden, F. Viel, T. McLaughlin, A. Jarandehei, M. Miller, D. Falconnet, A. K. White, D. G. Kent, M. R. Copley, F. Taghipour, C. J. Eaves, R. K. Humphries, J. M. Piret, and C. L. Hansen, "High-throughput analysis of single hematopoietic stem cell proliferation in microfluidic cell culture arrays," Nat. Methods **8**(7), 581–586 (2011).

[86] A. Bremer, T. Mittag, and M. Heymann, "Microfluidic characterization of macromolecular liquid-liquid phase separation," Lab Chip **20**(22), 4225–4234 (2020).

[87] A. Bouchaudy, C. Loussert, and J. B. Salmon, "Steady microfluidic measurements of mutual diffusion coefficients of liquid binary mixtures," AIChE J. **64**(1), 358–366 (2018).

[88] G. C. Randall and P. S. Doyle, "Permeation-driven flow in poly(dimethylsiloxane) microfluidic devices," Proc. Natl. Acad. Sci. U.S.A. **102**(31), 10813–10818 (2005).

[89] X. Noblin, L. Mahadevan, I. A. Coomaraswamy, D. A. Weitz, N. M. Holbrook, and M. A. Zwieniecki, "Optimal vein density in artificial and real leaves," Proc. Natl. Acad. Sci. U.S.A. **105**(27), 9140–9144 (2008).

[90] N. Ziane and J. B. Salmon, "Solidification of a charged colloidal dispersion investigated using microfluidic pervaporation," Langmuir **31**(29), 7943–7952 (2015).

[91] D. Garcia-Lojo, S. Gomez-Grana, V. F. Martin, D. M. Solis, J. M. Taboada, J. Perez-Juste, and I. Pastoriza-Santos, "Integrating plasmonic supercrystals in microfluidics for ultrasensitive, label-free, and selective surface-enhanced Raman spectroscopy detection," ACS Appl. Mater. Interfaces **12**(41), 46557–46564 (2020).

[92] J. Zhong, S. H. Zandavi, H. Li, B. Bao, A. H. Persad, F. Mostowfi, and D. Sinton, "Condensation in one-dimensional dead-end nanochannels," ACS Nano **11**(1), 304–313 (2017).

[93] Y. Shi, O. Ilic, H. A. Atwater, and J. R. Greer, "All-day fresh water harvesting by microstructured hydrogel membranes," Nat. Commun. **12**, 2797 (2021).

[94] M. Soltani and K. Golovin, "Lossless, passive transportation of low surface tension liquids induced by patterned omniphobic liquidlike polymer brushes," Adv. Funct. Mater. **32**(1), 2107465 (2022).

[95] C. H. Park, S. Y. Lee, D. S. Hwang, D. W. Shin, D. H. Cho, K. H. Lee, T. W. Kim, T. W. Kim, M. Lee, D. S. Kim, C. M. Doherty, A. W. Thornton, A. J. Hill, M. D. Guiver, and Y. M. Lee, "Nanocrack-regulated self-humidifying membranes," Nature **532**(7600), 480–483 (2016).

[96] J. de Jong, R. G. Lammertink, and M. Wessling, "Membranes and microfluidics: A review," Lab Chip **6**(9), 1125–1139 (2006).

[97] S. Schneider, D. Gruner, A. Richter, and P. Loskill, "Membrane integration into PDMS-free microfluidic platforms for organ-on-chip and analytical chemistry applications," Lab Chip **21**(10), 1866–1885 (2021).

[98] Y. Yuan, Z. Cui, H. Jia, and J. Wang, "High efficiency membrane technology in microfluidic systems," Sep. Purif. Rev. **51**(4), 545–562 (2022).

[99] J. G. Wijmans and R. W. Baker, "The solution-diffusion model: A review," J. Membr. Sci. **107**(1-2), 1–21 (1995).

[100] W. J. Koros and G. K. Fleming, "Membrane-based gas separation," J. Membr. Sci. **83**(1), 1–80 (1993).

[101] A. Lamberti, S. L. Marasso, and M. Cocuzza, "PDMS membranes with tunable gas permeability for microfluidic applications," RSC Adv. **4**(106), 61415–61419 (2014).

[102] E. Ricci, M. Minelli, and M. G. De Angelis, "Modelling sorption and transport of gases in polymeric membranes across different scales: A review," Membranes **12**(9), 857 (2022).

[103] L. M. Robeson, "Correlation of separation factor versus permeability for polymeric membranes," J. Membr. Sci. **62**(2), 165–185 (1991).

[104] L. M. Robeson, "The upper bound revisited," J. Membr. Sci. **320**(1-2), 390–400 (2008).

[105] A. O. Malakhov and V. V. Volkov, "Mixed-gas selectivity based on pure gas permeation measurements: An approximate model," Membranes **11**(11), 833 (2021).

[106] C. A. Scholes, S. Kanehashi, G. W. Stevens, and S. E. Kentish, "Water permeability and competitive permeation with $CO_2$ and $CH_4$ in perfluorinated polymeric membranes," Sep. Purif. Technol. **147**, 203–209 (2015).

[107] K. V. Otvagina, A. A. Atlaskin, M. M. Trubyanov, S. S. Kryuchkov, K. A. Smorodin, A. E. Mochalova, and I. V. Vorotyntsev, "Effect of moisture presence on gas permeability through gas separation membranes based on poly (vinyltrimethylsilane) and quaternized chitosan," Membr. Membr. Technol. **2**(2), 125–131 (2020).

[108] W. L. Robb, "Thin silicone membranes-their permeation properties and some applications," Ann. N.Y. Acad. Sci. **146**(1), 119–137 (1968).

[109] C. Makhloufi, D. Roizard, and E. Favre, "Reverse selective $NH_3/CO_2$ permeation in fluorinated polymers using membrane gas separation," J. Membr. Sci. **441**, 63–72 (2013).

[110] B. Nelson, M.S. thesis, Colorado School of Mines, 1997.

[111] G. Clarizia, C. Algieri, and E. Drioli, "Filler-polymer combination: A route to modify gas transport properties of a polymeric membrane," Polymer **45**(16), 5671–5681 (2004).

[112] S. A. Stern and B. D. Bhide, "Permeability of silicone polymers to ammonia and hydrogen sulfide," J. Appl. Polym. Sci. **38**(11), 2131–2147 (1989).

[113] T. C. Merkel, V. I. Bondar, K. Nagai, B. D. Freeman, and I. Pinnau, "Gas sorption, diffusion, and permeation in poly(dimethylsiloxane)," J. Polym. Sci. B: Polym. Phys. **38**(3), 415–434 (2000).

[114] Z. P. Smith, R. R. Tiwari, M. E. Dose, K. L. Gleason, T. M. Murphy, D. F. Sanders, G. Gunawan, L. M. Robeson, D. R. Paul, and B. D. Freeman, "Influence of diffusivity and sorption on helium and hydrogen separations in hydrocarbon, silicon, and fluorocarbon-based polymers," Macromolecules **47**(9), 3170–3184 (2014).

[115] L. Brandão, L. M. Madeira, and A. M. Mendes, "Mass transport on composite dense PDMS membranes with palladium nanoclusters," J. Membr. Sci. **288**(1-2), 112–122 (2007).

[116] S. Metz, W. Vandeven, J. Potreck, M. Mulder, and M. Wessling, "Transport of water vapor and inert gas mixtures through highly selective and highly permeable polymer membranes," J. Membr. Sci. **251**(1-2), 29–41 (2005).

[117] S. F. Timashev, A. V. Vorobiev, V. I. Kirichenko, Y. M. Popkov, V. I. Volkov, R. R. Shifrina, A. Y. Lyapunov, A. G. Bondarenko, and L. P. Bobrova, "Specifics of highly selective ammonia transport through gas-separating membranes based on perfluorinated copolymer in the form of hollow fibers," J. Membr. Sci. **59**(2), 117–131 (1991).

[118] T. C. Merkel and L. G. Toy, "Comparison of hydrogen sulfide transport properties in fluorinated and nonfluorinated polymers," Macromolecules **39**(22), 7591–7600 (2006).

[119] L. Ansaloni, R. Rennemo, H. K. Knuutila, and L. Deng, "Development of membrane contactors using volatile amine-based absorbents for $CO_2$ capture: Amine permeation through the membrane," J. Membr. Sci. **537**, 272–282 (2017).

[120] D. J. Branken, H. M. Krieg, J. P. le Roux, and G. Lachmann, "Separation of $NF_3$ and $CF_4$ using amorphous glassy perfluoropolymer teflon AF and Hyflon AD60 membranes," J. Membr. Sci. **462**, 75–87 (2014).

[121] T. C. Merkel, V. Bondar, K. Nagai, B. D. Freeman, and Y. P. Yampolskii, "Gas sorption, diffusion, and permeation in poly[2,2-bis(trifluoromethyl)-4,5-difluoro-1,3-dioxole-co-tetrafluoroethylene]," Macromolecules **32**(25), 8427–8440 (1999).

[122] Chemours, Teflon AF product information; see https://www.teflon.com/en/-/media/files/teflon/teflon-af-product-info.pdf; accessed 14 July 2023.

[123] J. C. Jansen, K. Friess, and E. Drioli, "Organic vapour transport in glassy perfluoropolymer membranes: A simple semi-quantitative approach to analyze clustering phenomena by time lag measurements," J. Membr. Sci. **367**(1-2), 141–151 (2011).

[124] I. Pinnau and L. G. Toy, "Gas and vapor transport properties of amorphous perfluorinated copolymer membranes based on 2,2-bistrifluoromethyl-4,5-difluoro-1,3-dioxole/tetrafluoroethylene," J. Membr. Sci. **109**(1), 125–133 (1996).

[125] S. M. Nemser and I. C. Roman, "Perfluorodioxole membranes," U.S. patent 5051114B2 (24 September 1991).

[126] P. Bian, Y. Wang, and T. J. McCarthy, "Rediscovering silicones: The anomalous water permeability of 'hydrophobic' PDMS suggests nanostructure and applications in water purification and anti-icing," Macromol. Rapid Commun. **42**(5), 2000682 (2021).

[127] K. Raj M and S. Chakraborty, "PDMS microfluidics: A mini review," J. Appl. Polym. Sci. **137**(27), 48958 (2020).

[128] R. Li, X. Guo, K. Xiong, X. Xing, and C. Zhang, "Microbial micro-tube culture system: A miniature bioreactor for controllable bubble-free oxygen supply based on high gas-permeability Teflon tube," Biochem. Eng. J. **191**, 108789 (2023).

[129] A. Tokarev, K. Friess, J. Machkova, M. Šipek, and Y. Yampolskii, "Sorption and diffusion of organic vapors in amorphous Teflon AF2400," J. Polym. Sci. B: Polym. Phys. **44**(5), 832–844 (2006).

[130] T. Masuda, Y. Iguchi, B. Z. Tang, and T. Higashimura, "Diffusion and solution of gases in substituted polyacetylene membranes," Polymer **29**(11), 2041–2049 (1988).

[131] S. G. Jennings, "The mean free path in air," J. Aerosol Sci. **19**(2), 159–166 (1988).

[132] H. Chamani, T. Matsuura, D. Rana, and C. Q. Lan, "Transport characteristics of liquid-gas interface in a capillary membrane pore," J. Membr. Sci. **611**, 118387 (2020).

[133] C. Liu, J. A. Thompson, and H. H. Bau, "A membrane-based, high-efficiency, microfluidic debubbler," Lab Chip **11**(9), 1688–1693 (2011).

[134] H. S. Rabbani, V. Joekar-Niasar, and N. Shokri, "Effects of intermediate wettability on entry capillary pressure in angular pores," J. Colloid Interface Sci. **473**, 34–43 (2016).

[135] A. Samadi, T. Ni, E. Fontananova, G. Tang, H. Shon, and S. Zhao, "Engineering antiwetting hydrophobic surfaces for membrane distillation: A review," Desalination **563**, 116722 (2023).

[136] T. Horseman, Y. Yin, K. S. S. Christie, Z. Wang, T. Tong, and S. Lin, "Wetting, scaling, and fouling in membrane distillation: State-of-the-art insights on fundamental mechanisms and mitigation strategies," ACS EST Eng. **1**(1), 117–140 (2021).

[137] Y. Gao, A. Montana, and F. Chen, "Evaluation of porosity and thickness on effective diffusivity in gas diffusion layer," J. Power Sources **342**, 252–265 (2017).

[138] M. W. Toepke and D. J. Beebe, "PDMS absorption of small molecules and consequences in microfluidic applications," Lab Chip **6**(12), 1484–1486 (2006).

[139] M. Badv, F. Bayat, J. I. Weitz, and T. F. Didar, "Single and multi-functional coating strategies for enhancing the biocompatibility and tissue integration of blood-contacting medical implants," Biomaterials **258**, 120291 (2020).

[140] J. H. Nam and M. Kaviany, "Effective diffusivity and water-saturation distribution in single- and two-layer PEMFC diffusion medium," Int. J. Heat Mass Transfer **46**(24), 4595–4611 (2003).

[141] J.-G. Choi, D. D. Do, and H. D. Do, "Surface diffusion of adsorbed molecules in porous media: Monolayer, multilayer, and capillary condensation regimes," Ind. Eng. Chem. Res. **40**(19), 4005–4031 (2001).

[142] J. Shen, G. Liu, Y. Han, and W. Jin, "Artificial channels for confined mass transport at the sub-nanometre scale," Nat. Rev. Mater. **6**(4), 294–312 (2021).

[143] Q. Qian, P. A. Asinger, M. J. Lee, G. Han, K. Mizrahi Rodriguez, S. Lin, F. M. Benedetti, A. X. Wu, W. S. Chi, and Z. P. Smith, "MOF-based membranes for gas separations," Chem. Rev. **120**(16), 8161–8266 (2020).

[144] S. T. Oyama, M. Yamada, T. Sugawara, A. Takagaki, and R. Kikuchi, "Review on mechanisms of gas permeation through inorganic membranes," J. Jpn. Pet. Inst. **54**(5), 298–309 (2011).

[145] S. Bandehali, A. Ebadi Amooghin, H. Sanaeepur, R. Ahmadi, A. Fuoco, J. C. Jansen, and S. Shirazian, "Polymers of intrinsic microporosity and thermally rearranged polymer membranes for highly efficient gas separation," Sep. Purif. Technol. **278**, 119513 (2021).

[146] W. H. Lee, J. G. Seong, X. Hu, and Y. M. Lee, "Recent progress in microporous polymers from thermally rearranged polymers and polymers of intrinsic microporosity for membrane gas separation: Pushing performance limits and revisiting trade-off lines," J. Polym. Sci. **58**(18), 2450–2466 (2020).

[147] T. Han, Z. Cai, C. Wang, P. Zheng, Q. Wu, L. Liu, X. Liu, J. Weidman, and S. Luo, "Ionic microporous polymer membranes for advanced gas separations," Ind. Eng. Chem. Res. **62**(4), 1764–1775 (2023).

[148] C. Z. Liang, T.-S. Chung, and J.-Y. Lai, "A review of polymeric composite membranes for gas separation and energy production," Prog. Polym. Sci. **97**, 101141 (2019).

[149] H. B. Tanh Jeazet, C. Staudt, and C. Janiak, "Metal-organic frameworks in mixed-matrix membranes for gas separation," Dalton Trans. **41**(46), 14003–14027 (2012).

[150] J. H. Kim, S. J. Moon, S. H. Park, M. Cook, A. G. Livingston, and Y. M. Lee, "A robust thin film composite membrane incorporating thermally rearranged polymer support for organic solvent nanofiltration and pressure retarded osmosis," J. Membr. Sci. **550**, 322–331 (2018).

[151] D. Fritsch, P. Merten, K. Heinrich, M. Lazar, and M. Priske, "High performance organic solvent nanofiltration membranes: Development and thorough testing of thin film composite membranes made of polymers of intrinsic microporosity (PIMs)," J. Membr. Sci. **401-402**, 222–231 (2012).
[152] M. Qu, O. Abdelaziz, Z. Gao, and H. Yin, "Isothermal membrane-based air dehumidification: A comprehensive review," Renew. Sust. Energy Rev. **82**, 4060–4069 (2018).
[153] T.-V. Dinh, I.-Y. Choi, Y.-S. Son, and J.-C. Kim, "A review on non-dispersive infrared gas sensors: Improvement of sensor detection limit and interference correction," Sens. Actuators B **231**, 529–538 (2016).
[154] M. Liu, L. Wang, X. Zheng, and Z. Xie, "Zirconium-based nanoscale metal-organic framework/poly(epsilon-caprolactone) mixed-matrix membranes as effective antimicrobials," ACS Appl. Mater. Interfaces **9**(47), 41512–41520 (2017).
[155] T. D. Wheeler and A. D. Stroock, "The transpiration of water at negative pressures in a synthetic tree," Nature **455**(7210), 208–212 (2008).
[156] L. Guo, Y. Liu, L. Liu, P. Yin, C. Liu, and J. Li, "Study of the mechanism of embolism removal in xylem vessels by using microfluidic devices," Lab Chip **23**(4), 737–747 (2023).